A Metapopulation Network Model for the Spreading of SARS-CoV-2: Case Study for Ireland

Rory Humphries,[1,*] Mary Spillane,[1,†] Kieran Mulchrone,[1,‡] Sebastian Wieczorek,[1,§] Micheal O'Riordain,[1,2,¶] and Philipp Hövel[1,**]

[1] *School of Mathematical Sciences, University College Cork, Western Road, Cork T12 XF64, Ireland*

[2] *Department of Surgery, Mercy University Hospital, Grenville Place, Cork, T12 WE28, Ireland*

(Dated: July 11, 2020)

Abstract

We present preliminary results on an all-Ireland network modelling approach to simulate the spreading the Severe Acute Respiratory Syndrome CoronaVirus 2 (SARS-CoV-2), commonly known as the *coronavirus*. In the model, nodes correspond to locations or communities that are connected by links indicating travel and commuting between different locations. While this proposed modelling framework can be applied on all levels of spatial granularity and different countries, we consider Ireland as a case study. The network comprises 3440 *electoral divisions* (EDs) of the Republic of Ireland and 890 *superoutput areas* (SOAs) for Northern Ireland, which corresponds to local administrative units below the NUTS 3 regions. The local dynamics within each node follows a phenomenological SIRX compartmental model including classes of Susceptibles, Infected, Recovered and Quarantined (X) inspired from Science **368**, 742 (2020). For better comparison to empirical data, we extended that model by a class of Deaths. We consider various scenarios including the 5-phase roadmap for Ireland. In addition, as proof of concept, we investigate the effect of dynamic interventions that aim to keep the number of infected below a given threshold. This is achieved by dynamically adjusting containment measures on a national scale, which could also be implemented at a regional (county) or local (ED/SOA) level. We find that – in principle – dynamic interventions are capable to limit the impact of future waves of outbreaks, but on the downside, such a strategy can last several years until herd immunity will be reached.

* r.humphries@umail.ucc.ie
† mary.spillane@umail.ucc.ie
‡ k.mulchrone@ucc.ie
§ sebastian.wieczorek@ucc.ie
¶ micheal.oriordain@ucc.ie
** philipp.hoevel@ucc.ie

The model proposed in this discussion paper and the numerical results arising from it are to be understood as a contribution to the scientific and public discussion of possible spreading scenarios and the impact of interventions measures. We will clearly state the model ingredients and assumptions and elaborate on conclusions that can be drawn based on these limitations; some of which are unlikely for any practical purpose, but worth exploring, e.g., for worst-case scenarios.

After the introduction and discussion of the model equations for the local and networked dynamics in sections I and II, respectively, we continue with a case study of Ireland in section III. Besides an unlikely, worst-case scenario, we consider different levels of increased awareness during the post lock-down period in section III B. In addition, in section III C, we explore effects of dynamic interventions to keep the prevalence below a given level.

I. LOCAL DYNAMICS

We start with the model for the local, well mixed dynamics at a single node as the basis for the network model:

$$\dot{S} = -\beta c \frac{SI}{N} \tag{1a}$$

$$\dot{I} = \beta c \frac{SI}{N} - \mu I - \alpha I - \kappa I \tag{1b}$$

$$\dot{X} = \kappa I - \mu X - \alpha X \tag{1c}$$

$$\dot{R} = \mu I + \mu X \tag{1d}$$

$$\dot{D} = \alpha I + \alpha X. \tag{1e}$$

The above model is a simple extension of the original Kermack and McKendrick SIR model [1], inspired by Ref. [2]. There are five compartments, N individuals, and each individual may belong to just one compartment at any time:

Susceptible $S(t)$**:** Individuals who have not been infected by the disease.

Infected $I(t)$**:** Individuals who are infected with the disease and are capable of transmission.

Quarantined $X(t)$**:** Individuals who are infected with the disease, but are quarantined or self-isolating and thus not transmitting.

Recovered $R(t)$**:** Individuals who have recovered from the disease and are considered immune.

Dead $D(t)$**:** Individuals who have died from the disease.

The above system of ordinary differential equations (ODEs) assume homogeneous mixing of the population, which can be a good approximation for small communities, and small number of deaths. The parameters of the ODE model (1) refer to the rates of moving from one compartment to another and population size:

β**:** probability of infection on contact.

c: rate of contact/mixing.

μ: rate of recovery.

κ: rate of moving from infected to quarantined.

α: rate of death.

N: total population size $N = S(t) + I(t) + X(t) + R(t) + D(t) = \text{const.}$.

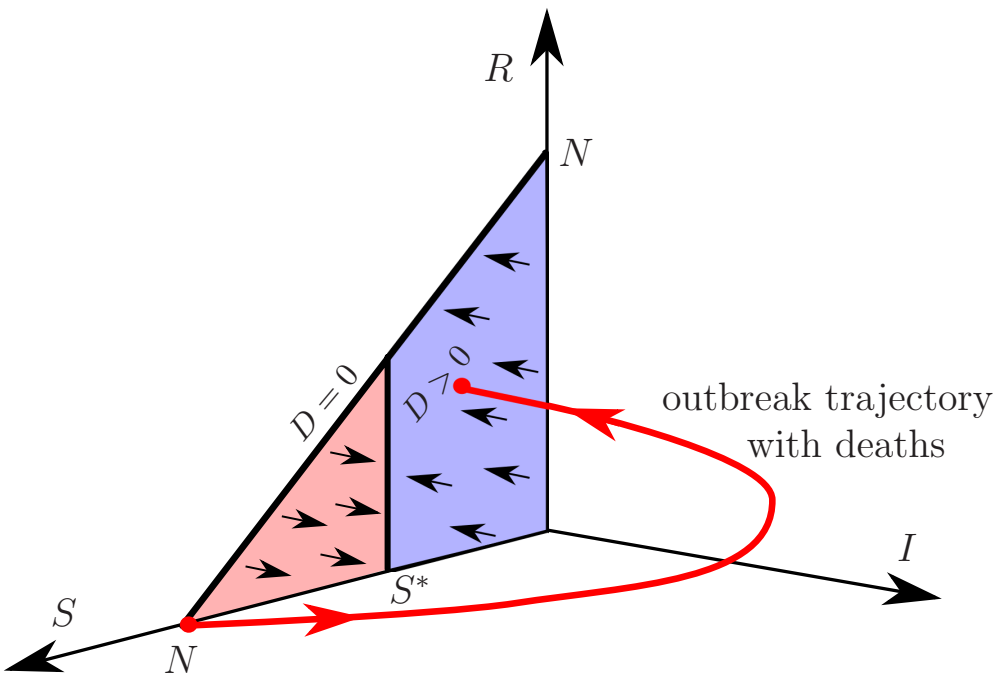

FIG. 1: Sketch of the outbreak dynamics in the local SIXRD model (1) for $R_0 > 1$, shown as a (red) trajectory from the disease-free equilibrium $S_e = N$ to one of the stable equilibria with $0 < S_e < S^*$ in the projection of the (S, I, X, R, D) phase space onto the (S, I, R) subspace. S^* is the herd immunity threshold separating the triangular family of equilibria into the (pink) unstable and (blue) stable parts.

Much insight into the network dynamics can be gained from geometric analysis of the local, single-node dynamics. In the (S, I, X, R, D) phase space, system (1) has a whole family of stationary solutions (equilibria), which are given by

$$I_e = X_e = 0 \quad \text{and} \quad S_e + R_e + D_e = N, \tag{2}$$

and form a triangular surface shown in Fig. 1. This family includes the important disease-free equilibrium $S_e = N, I_e = X_e = R_e = D_e = 0$. To discuss stability of equilibria, it is convenient to introduce the *basic reproduction number*:

$$R_0 = \frac{\beta\, c}{\alpha + \kappa + \mu}. \tag{3}$$

When $0 < R_0 < 1$, all equilibria are stable, meaning that no disease outbreaks can occur. When $R_0 = 1$, the disease-free equilibrium turns unstable. When $R_0 > 1$, disease outbreaks become possible. To be more specific, the family of equilibria is divided into the (pink)

unstable part with $S^* < S_e \leq N$, which contains the disease-free equilibrium, and the (blue) stable part with $0 \leq S_e < S^*$, shown in Fig. 1. The instability threshold separating the two parts is given by

$$S^* = \frac{N}{R_0}. \tag{4}$$

Guided by these observations, we define *herd immunity* as follows:

Definition. *In the local SIXRD model* (1)*, we define* herd immunity *as a state of the system with low enough level of susceptible S so that no outbreaks can occur upon a small increase in infected I:*

$$0 < S < S^* \quad \textit{and} \quad I = X = 0.$$

We call $S^* = N/R_0$ the herd immunity threshold.

In Fig. 1, a disease outbreak is represented by the (red) trajectory from the disease-free equilibrium, giving a peak in infected $I(t)$ around the herd immunity threshold S^*, to one of the (blue) herd immunity equilibria that lie below S^*. The lower the S^*, the higher the peak in $I(t)$. Bringing the herd immunity threshold S^* closer to N for a period of time, e.g. via imposing Public Health restrictions, can modify the outbreak trajectory so that ultimate herd immunity is achieved with a peak in $I(t)$ that remains below some desired level.

II. NETWORK MODEL

While the ODE model (1) can be justified for small communities, it fails at capturing the dynamics that occurs at large spatial scales and cannot account for heterogeneities in a population and interaction between metapopulations via mixing/commuting [3]. For this reason, we develop a network framework by splitting the population up into a number of smaller communities based on their geographic location. Ideally, these communities are small enough to justify a well mixed ODE model at the local level.

Every community corresponds to a node in the network. Two nodes are connected by a link, which represent the number of people travelling between the involved communities. The number of people travelling can vary with time or remain static. The resulting network model is given by

$$\begin{aligned}
\dot{S}_i =& -\beta c \left(S_i - \sum_j S_{ij} \right) \frac{I_i + \sum_k (I_{ki} - I_{ik})}{N_i + \sum_k (N_{ki} - N_{ik})} \\
& - \beta c \sum_j S_{ij} \frac{I_j + \sum_k (I_{kj} - I_{jk})}{N_j + \sum_k (N_{kj} - N_{jk})} && \text{(5a)} \\
\dot{I}_i =& \beta c \left(S_i - \sum_j S_{ij} \right) \frac{I_i + \sum_k (I_{ki} - I_{ik})}{N_i + \sum_k (N_{ki} - N_{ik})} \\
& + \beta c \sum_j S_{ij} \frac{I_j + \sum_k (I_{kj} - I_{jk})}{N_j + \sum_k (N_{kj} - N_{jk})} - \mu I - \alpha I - \kappa I && \text{(5b)} \\
\dot{X}_i =& \kappa I_i - \mu X_i - \alpha X_i && \text{(5c)} \\
\dot{R}_i =& \mu I_i + \mu X_i && \text{(5d)} \\
\dot{D}_i =& \alpha I_i + \alpha X_i. && \text{(5e)}
\end{aligned}$$

For notational convenience, the compartments are now labelled by a subscript, i.e., S_i, I_i, X_i, R_i, and D_i, to denote the number of individuals belonging to the respective compartments of i-th node in the network ($S_i + I_i + X_i + R_i + D_i = N_i$). Similarly, the number of individuals travelling from node i to node j belonging to a given compartment is denoted by $S_{ij}, I_{ij}, X_{ij}, R_{ij}$, and D_{ij} resulting in $N_{ij} = S_{ij} + I_{ij} + X_{ij} + R_{ij} + D_{ij}$.

Note that the network model includes interactions between nodes only in the susceptible and infected compartments. Accordingly, we account for the number of (i) individuals that remain in their home node and (ii) those who travel to other nodes in the first and second term of Eqs. (5a) and (5b), respectively.

Given a number of travellers N_{ij} between nodes, the network model (5) assumes that the number of travellers belonging to the respective compartments is determined by a relation such as $S_{ij} = N_{ij}\frac{S_i}{N_i}$. Thus, the number of travelling susceptibles is proportional to the number of susceptibles in the home node. The number of travelling individuals in the other compartments is computed in the same fashion.

N_{ij} may be randomly generated at each time step. The distance travelled between locations often follows a power-law or heavy-tail distribution and can be described by a gravity or radiation population model [4–9]. Alternatively, empirical movement data can inform the model. From these data one can either build a static network using, e.g., the jump-size distributions, or randomly generate a network at each time-step. Note that the proposed network model does not account for any importation from outside Ireland.

For the fully networked case [cf. Eqs.(5)], the basic reproduction number R_0 can be computed from the system's next generation matrix [10]. this takes into account the couplings between the nodes when computing the stability of the disease-free equilibrium. The (i, j) entry of this matrix, which we denote G, gives the expected number of new infections in node i caused by an infected individual introduced in node j. The next generation matrix, as derived in Appendix A, is given as

$$G_{ij} = \frac{\beta c}{\mu + \alpha + \kappa}\left[\left(S_i - \sum_k S_{ik}\right)\frac{\delta_{ij}\left(1 - \sum_k \frac{N_{ik}}{N_i}\right) + \frac{N_{ji}}{N_j}}{N_i + \sum_k (N_{ki} - N_{ik})} + \sum_k S_{ik}\frac{\delta_{jk}\left(1 - \sum_l \frac{N_{jl}}{N_j}\right) + \frac{N_{jk}}{N_j}}{N_k + \sum_l (N_{lk} - N_{kl})}\right] \tag{6}$$

Then, the reproduction number R_0 is given by the spectral radius ρ of the the next generation matrix,

$$R_0 = \rho(G). \tag{7}$$

This provides a condition necessary for the stability all disease-free equilibria ($I_i = X_i = 0, S_i + R_i + D_i = N_i \quad \forall i$). It also gives a natural definition for herd immunity in the network, as the networked reproduction number R_0 is now a function of all susceptible populations (cf. the definition of heard immunity for the local dynamics in Sec. I).

All scenarios discussed in the next sections are simulated using our library for modelling epidemics on networks, EpiGraph [11], which is implemented in C++ and freely available on GitHub.

III. CASE STUDY: IRELAND

For the remainder of this discussion paper, we elaborate on the spreading of SARS-CoV-2 in Ireland as a case study. The network model given by Eqs. (5) is informed by publicly

Phase	Mobility	Social distancing
pre lock-down	no restrictions	no restrictions
initial lock-down	travel with 2km radius	essential meetings only
1	travel with 5km radius	essential meetings only
2	travel with 20m radius	maximum of 4 people
3	travel with 20km radius	maximum of 4 people
4	no restrictions	small gatherings
5	no restrictions	large gatherings
post lock-down	no restrictions	no restrictions

TABLE I: Travel and gathering restrictions during the 5 phases of the Irish roadmap.

available data detailed in the next section.

A. Network Data

For the Republic of Ireland, each of the 3440 nodes in the network represents an *electoral division* as defined by the central statistics office (CSO), for which small area population statistics are published from the 2016 census. [12]. The links in the network are the number of commuters between each electoral division according to CSO data [13]. Similarly, for Northern Ireland, nodes refer to 890 *superoutput areas* according to Northern Ireland Statistics and Research Agency (NISRA) [14]. This spatial resolution corresponds to the local administrative units below the category-3 regions of the *Nomenclature of Territorial Units for Statisticss* (NUTS) [15].

B. 5-Phase Roadmap without Additional Countermeasures

In order to demonstrate the general feasibility of the proposed modelling framework, we consider the 5-phase *roadmap for reopening society & business* by reducing lock-down restrictions as outlined by the Irish Government [16].

Our model attempts to follow the historic evolution of the disease up until phase 2. Then, we allow the model to run under the predicted affects of the remaining lock-down phases. See Tab. I for implications on travel and gathering restrictions. It is important to note that at this stage, we do not consider any reintroduction or roll back to earlier phases during the course of the simulated outbreak. This corresponds to a worst-case scenario and is highly unlikely from a practical point of view, because interventions will be reintroduced, if case numbers rise again.

The parameters are chosen such that it matches the actual number of deaths in Ireland. See Tab. II for details. It is important to note, however, that this model is in the early stages of testing and has not undergone any sensitivity training on the parameters. The effective infection probability β_{eff} is computed as $\beta_{\text{eff}} = \beta c$. As defined in Eq. (3), the basic reproduction number of the local dynamics [cf. Eqs. (1)] exceeds the critical value of $R_0^{\text{crit}} = 1$ during pre lock-down and after phase 3. Conversely, only initial lock-down, phases 1 and 2 have a R_0 value well below unity and – neglecting network-related effects – exhibit a burn out of an outbreak and self-guided decrease of the number of infected.

Phase	β	c	μ	κ	α	β_{eff}	R_0
pre lock-down	0.37	1	0.1	0.1	0.0028	0.37	1.82
initial lock-down	0.37	0.4	0.1	0.1	0.0028	0.15	0.73
1	0.37	0.3	0.1	0.1	0.0028	0.11	0.55
2	0.37	0.4	0.1	0.1	0.0028	0.15	0.73
3	0.37	0.5	0.1	0.1	0.0028	0.19	0.91
4	0.37	0.6	0.1	0.1	0.0028	0.22	1.09
5	0.37	0.7	0.1	0.1	0.0028	0.26	1.28
post lock-down	0.37	1	0.1	0.1	0.0028	0.37	1.82

TABLE II: Parameters for the 5 phases of the Irish roadmap. β_{eff} and R_0 are computed from the system parameters.

We introduce a small number of diseased individuals to the Dublin area on the 22nd of January, that is, 50 days before the initial lock-down, and run the model such that the disease spreads unimpeded. On the 12th of March, we introduce the initial lock-down measures, which take some time to reach full effect. Individuals' movement is limited to 2km and this is adhered to with 80% compliance. This level of compliance is supported by preliminary findings of a nation-wide series of phone interviews accounting for essential/justified and non-essential travel [17]. We account for social-distancing and self-isolation (X compartment) by reducing the rate of mixing c within communities (cf. Tab. II for the respective parameter values). During phases 1 and 2/3, the travel radius increased to 5km and 20km, respectively, and we assume the same level of compliance. Travel restrictions are removed in phases 4 and 5 (cf. Tab. I). Each of the numbered phases have a duration of 21 days.

Figures 2 depicts the time series of all five compartments – aggregated over all nodes – in semi-logarithmic scale. One can see two distinct peaks: (i) a small peak that occurs before the lock-down and (ii) a second peak that occurs once all lock-down measures are lifted. It is clear that unless some of the measure are maintained, then the lock-down will just have the effect of delaying the epidemic and result in a second wave with a prevalence that – in this unrealistic worst-case scenario – is 100 times higher than the first one and exceeds any realistic capacity of the health-case system. The number of infected eventually reaches zero due to a depletion of the pool of susceptibles. Following the geometric analysis of the local dynamics (cf. Sec. I), the trajectory lands at one of disease-free equilibria $I_{\text{e}} = 0$. A change in parameters, e.g., rate of mixing c, or a rescaling of the population to the number of remaining susceptibles can render this state unstable again. Then, a perturbation to the networked system, for instance, introduction or importation from outside, has the potential to trigger an additional outbreak.

As stated above, the parameters are chosen to match the actual number of deaths in Ireland. This, in turn, results in a larger first peak compared to the reported numbers of confirmed cases on the 12th of March ranging from 27 according to [18] to 70 according to [19] The simulated results, however, are not meant to reflect this range of confirmed cases, but following the logic of the model, refer to all infected individuals including asymptomatic, non-diagnosed and untested.

Figure 3a and 3b show spatially resolved snapshots of the prevalence of the disease per km^2 at times $t = 50$d (March 12) and $t = 320$d (December 7), respectively (cf. [20] for a map based on data of reported, confirmed cases). Figure 3a corresponds to the disease prevalence at the first peak before the lock-down. The disease remains in the East of the country for the most part with the exception of big towns and cities. In contrast, at $t = 320$d (Fig. 3b),

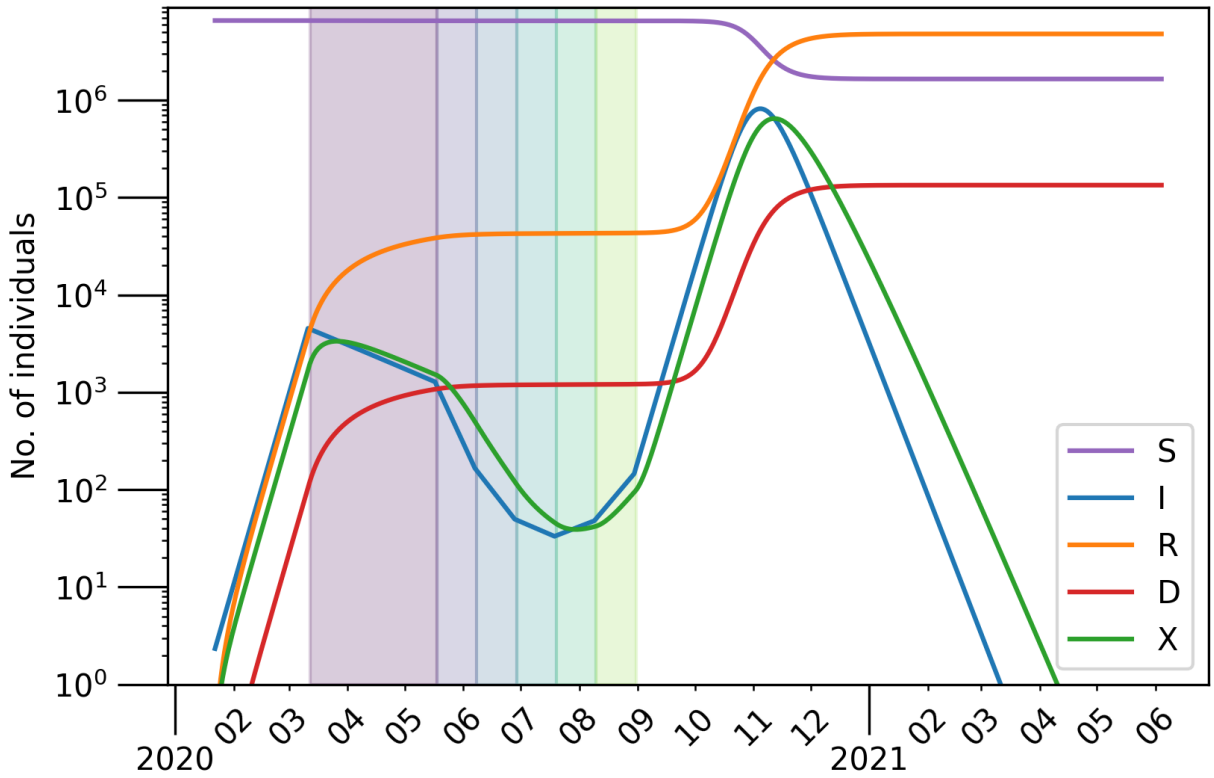

FIG. 2: Number of individuals (aggregated over the entire population/network) belonging to each compartment as stated in the legend over time with a log scale on the y-axis. Parameters as in Tab. II. Each successive lock-down phase is indicated by the differently colored shaded regions on the plot. After the initial lock-down (violet), phases 1 – 5 last 3 weeks each.

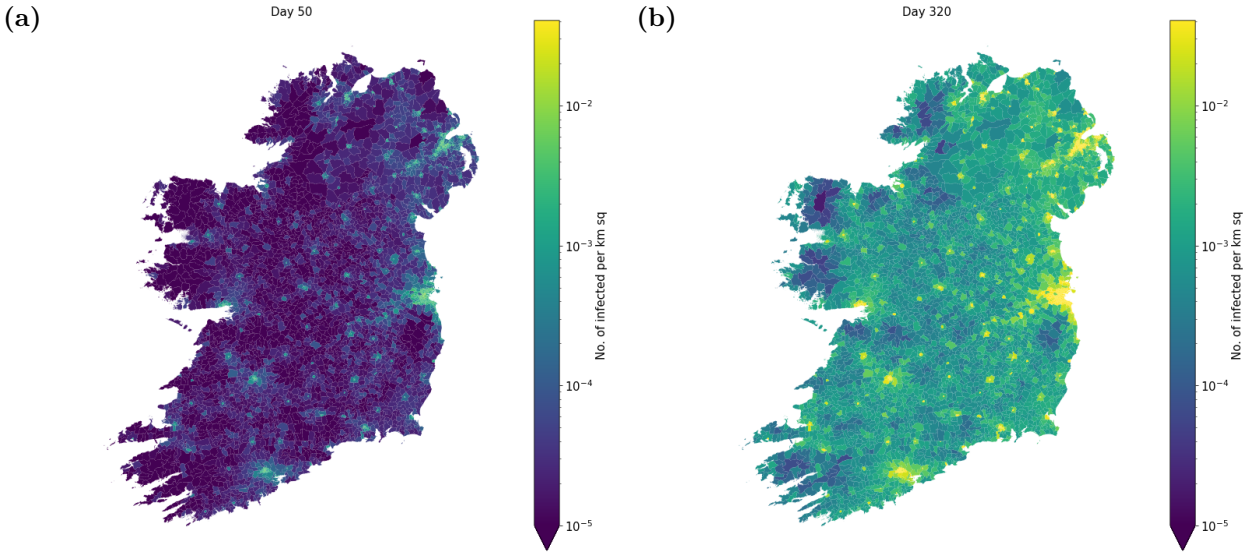

FIG. 3: The spatial distribution of infected individuals per km^2 around the two distinct peaks shown in Fig. 2 at (a) Day 50 (b) Day 320. Parameters as in Tab. II.

the outbreak covers the entire country and affects every electoral division. See Fig. 2 for a full time series of the aggregated variables.

Figure 4 shows the effect of different levels of awareness during the post lock-down phase,

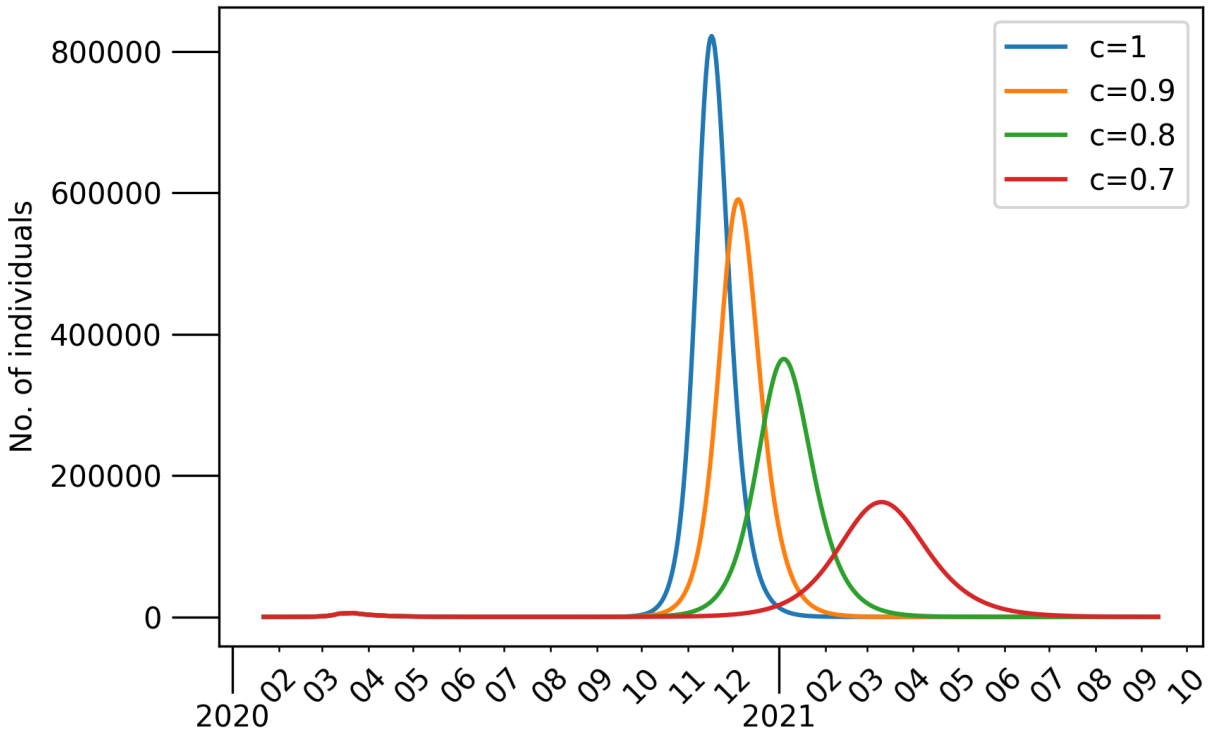

FIG. 4: Evolution of the aggregated, infected compartment I for varied post lock-down conditions. The blue curve corresponds to the parameters given in Tab. II (cf. Fig. 2 for a semi-logarithmic scale). The other curves vary the parameter c in the post lock-down phase as stated in the legend: $c = 0.9$, $c = 0.8$ and $c = 0.7$.

which is modelled by different values for the mixing parameter c. For convenience, the plots only depict the time series of the aggregated infected compartment I in a linear scale. A reduction to 70% of the original probability of infection significantly leads to a significantly smaller and delayed second peak (red curve), while the basic reproduction number of the local dynamics remains above unity (cf. Tab. II).

Similarly to Figure 4, the network model (5) allows considering different levels of compliance with travel restrictions. The effect is exemplified for aggregated values of I, X and D in Fig. 5 for compliance of 80% (solid curves, cf. Fig. 2) and 70% (dashed curves). One can see that for lower compliance, the second peak occurs earlier and has a higher amplitude. This results in a slightly increased number of deaths.

In order to show how the heavy-tail distribution of travel across the network causes a lack of sensitivity in initial conditions, we run the model for a number of random initial seeds where for each run only a single individual in one electoral division or superoutput area. The resulting time series are shown in Fig. 6.

One can see that both amplitude and timing of the large, second peak are stable and it is impossible to visually differentiate between any of the curves for different initial conditions. In the presented 4 cases, the initial location is selected uniformly at random from all network nodes. We note that deliberately selecting urban or rural locations will have no qualitative impact. To further corroborate the results, initial infections of a significant, finite fraction of the population will be explored. This might account for a considerable amount of unreported cases at the start of the recording of SARS-CoV-2 cases.

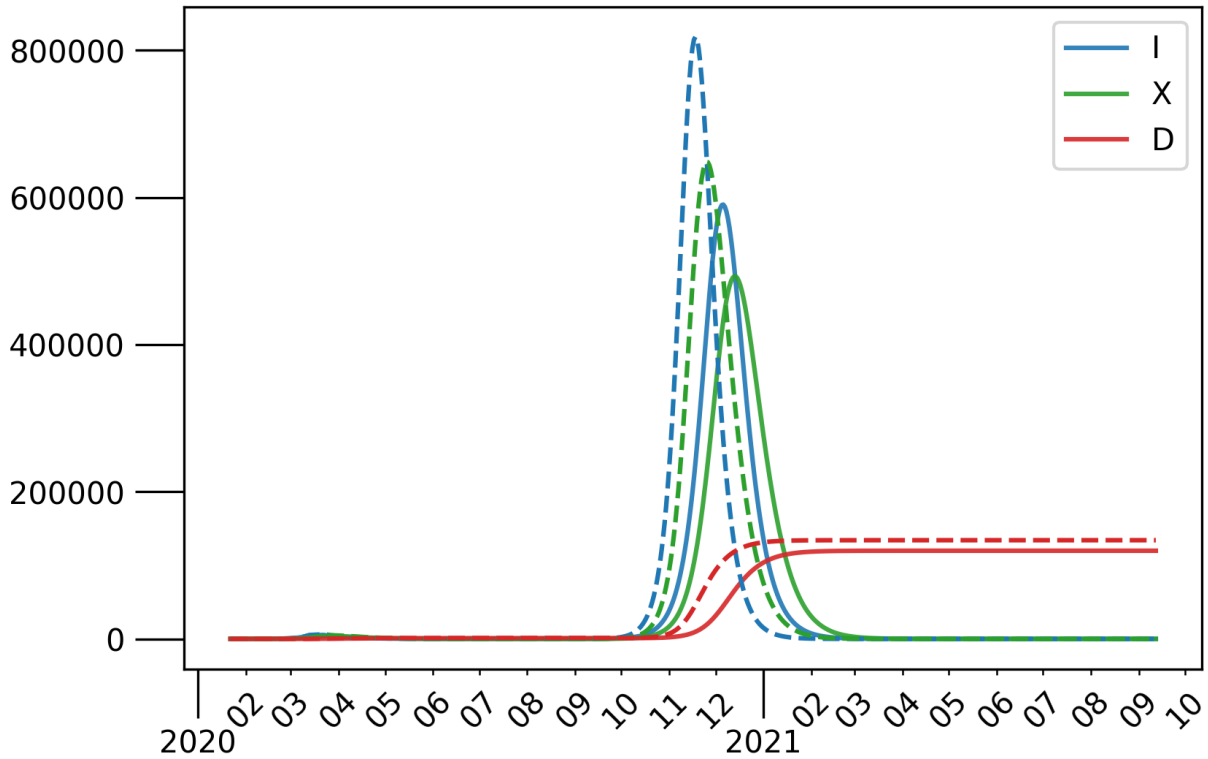

FIG. 5: Evolution of the aggregated, infected I (blue), quarantined X (green) and deceased D (red) compartments for two level of compliance with lock-down restrictions: 80% (solid, cf. Fig. 2), and 70% (dashed). Other parameters as in Tab. II.

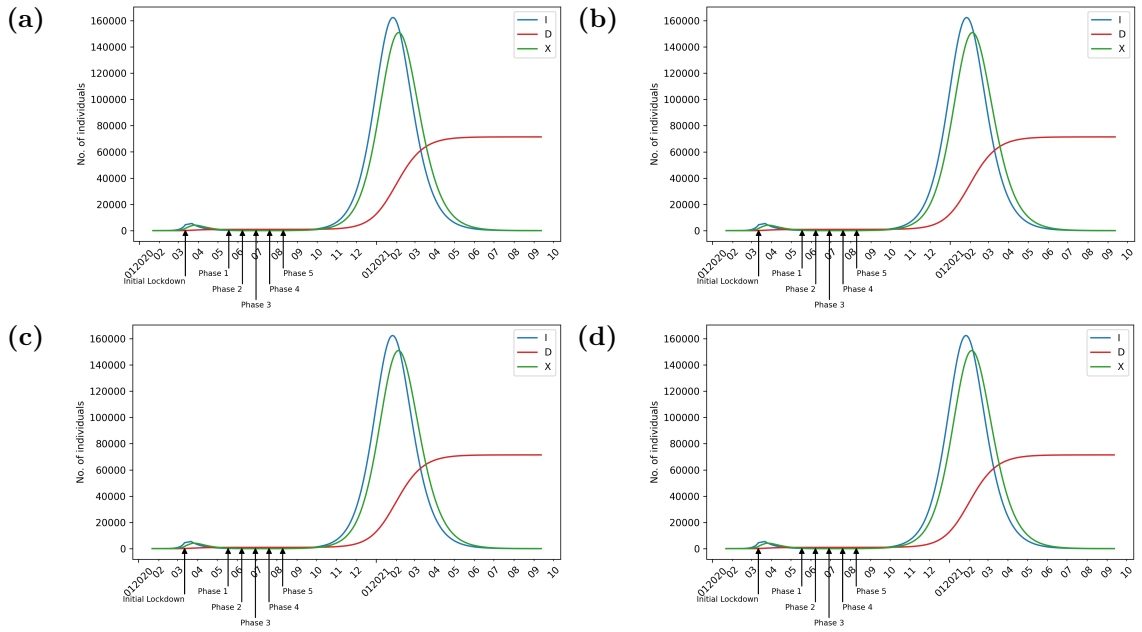

FIG. 6: Time series for 4 random initial conditions. Parameters as in Tab. II with $c = 0.7$ in the post lock-down period.

C. Dynamic Interventions

Finally, we discuss the likely scenario of a flexible lock-down policy that monitors to the prevalence of the disease within the island and aims to keep it below the capacity of the health-care system. As a simple measure, we define some threshold I_{th} as the maximum number of infected that can be present before we go back into lock-down and go through earlier phases again. Such a procedure corresponds to dynamic [21–23] or active [24] interventions. Specifically, we simulate until phase 3 as before to maintain the agreement with reported cases. Afterwards, if the condition $I_{\text{th}} > \sum_i I_i$ is met, the system goes back to phase 1 and then progresses from there until the condition is met again.

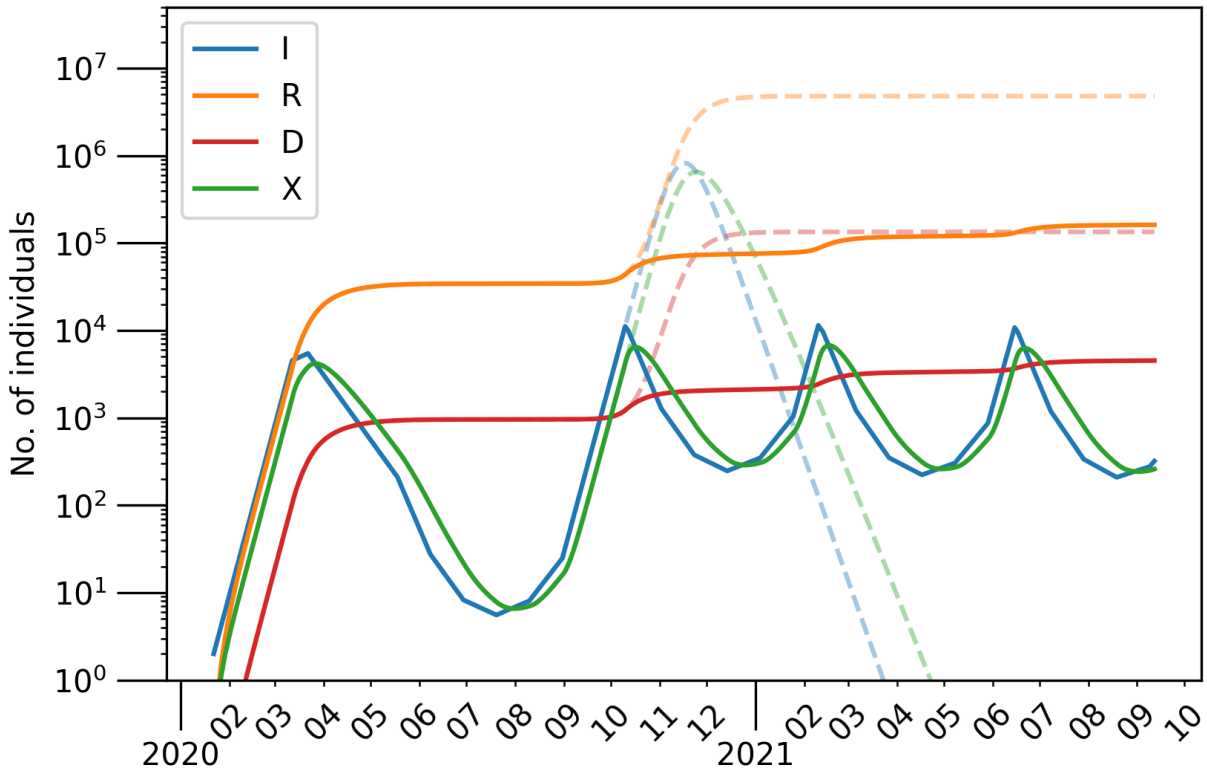

FIG. 7: The number of individuals belonging to each compartment over time (using the parameters in Tab. II) under a dynamic lock-down strategy taking $I_{\text{th}} = 10^4$. The dashed lines are the equivalent model without the dynamic lock-down strategy shown in Fig. 2.

In detail, we consider two scenarios with different threshold parameters, which are inspired by the reported, maximum number of hospitalized cases during the first wave in April 2020[25]: (i) $I_{\text{th}} = 10^4$, as shown in Fig. 7 and (ii) $I_{\text{th}} = 10^3$ as depicted in Fig. 8. In both figures, the worst-case scenario of Fig. 2 is added as dashed curves. Note that the curves of recovered R (orange) and deaths D (red) are only increasing at a low rate. For the case of $I_{\text{th}} = 10^4$, for instance, these values arrive at 10^5 after two years and thus, way below any effect of herd immunity.

Under the assumptions the considered network model, it would take many years for a significant depletion of the pool of susceptibles. Extrapolating from an extended run of the model similar to Fig. 7, we find that it would take roughly 27 years for the number of recovered to reach half the population, leading to a total number of approximately 92,000

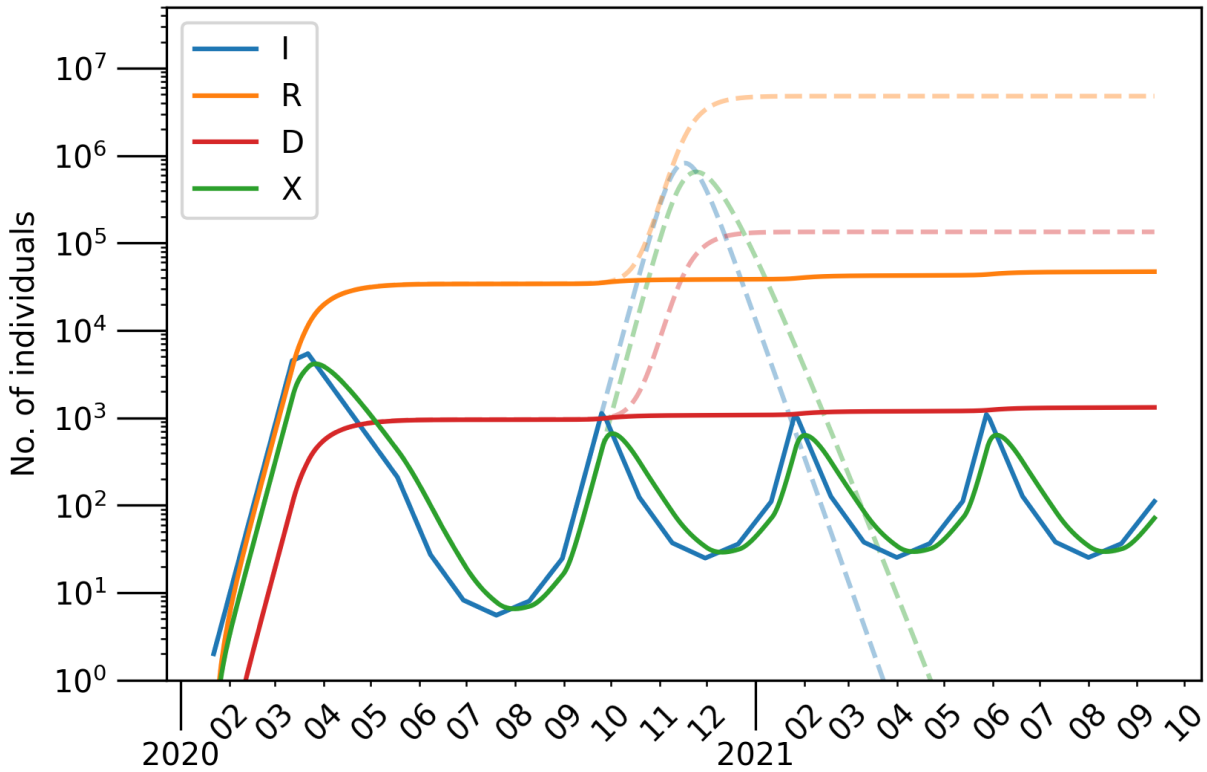

FIG. 8: The number of individuals belonging to each compartment over time (using the parameters in table II) under a dynamic lock-down strategy taking $I_{\rm th} = 10^3$. The dashed lines are the equivalent model without the dynamic lock-down strategy shown in Fig. 2.

deaths over the course of many waves. Even with a large threshold $I_{\rm th} = 10^4$ for the maximum number of infected cases, the feasibility of such a strategy is questionable due to the time it would take to reach herd immunity of on the island.

The re-introduction of lock-down measures to account for rising numbers of infected can change the stability of the disease-free equilibria $I_{\rm e} = 0$. However, as soon as the restrictions are relaxed, e.g., during phases 3 to 5, an unstable family of these equilibria re-emerges and the outbreak pattern repeats.

Suppressing the occurrence of unstable disease-free equilibria requires other forms of interventions. One could consider, for example, a fishing-type extension of the model [26–28]. This will basically turn the rate κ in the local dynamics (1) into a function of the number of infected. e.g., $\kappa(I) = \frac{h}{1+I/I_c}$ with a consumption/fishing rate h (here: rate of isolation) and a reference capacity I_c for $\kappa(I) = h/2$. This I dependence will account for contact-tracing effects, which are especially effective for low numbers of infected. As a consequence, a high rate h of isolation will be able to push the basic reproduction number R_0 [cf. Eq. (3)] below the critical value of $R_0^{\rm crit} = 1$ and change the stability of the equilibria $I_{\rm e} = 0$.

IV. CONCLUSION

We have proposed a dynamical network model to study the spreading of SARS-CoV-2 that accounts for travel/commuting between nodes of the network. As a case study, we have presented results from numerical simulations for Ireland, where the model is informed

from publicly available data on geographical regions, population, and mobility in both the Republic of Ireland and Northern Ireland. The network model is flexible in terms of spatial granularity and parameter selection. We have focused on the governmental 5-phase roadmap for reopening society & business and considered different initial conditions and parameters. We have observed that the roadmap will lead to a decline of case numbers. However, once the restrictions are lifted, the numbers will rise again, even if an increased level of awareness is considered. Finally, we have elaborated on a procedure of dynamic interventions that re-introduce lock-down measures, if a certain threshold of infected is reached. Following such a protocol, the overall number of infected can be controlled and safely kept below a prescribed threshold, which can be selected according to the capacity of the health-care system. We have considered that containment measures would be re-introduced on a country-wide level, but a more regional approach (county level) appears feasible as well. In any case, while the outbreak can be managed by dynamic interventions, it might take a period of several years until a significant fraction of the population will have lived through the disease and – under the assumption of immunity – and will have led to an effect of herd immunity.

Let us finish by stressing again that the times series and maps are preliminary findings and subject to a systematic sensitivity analysis. Nonetheless, we hope that the results presented in this discussion paper will stimulate scientific and public discussion about the purpose and effect of lock-down measures in the months ahead.

ACKNOWLEDGMENTS

The work is supported by Health Research Board Ireland in the framework of the COVID19 rapid response programme (grant number: COV19-2020-117). We are grateful to Andreas Amann, Patricia Kearny, Gerry Kileen, and Ivan Perry for helpful discussions.

---

[1] W. O. Kermack and A. G. McKendrick, Proc. R. Soc. A **115**, 700 (1927).
[2] B. F. Maier and D. Brockmann, Science **368**, 742 (2020).
[3] V. Belik, T. Geisel, and D. Brockmann, Phys. Rev. X **1**, 011001 (2011).
[4] D. Brockmann, L. Hufnagel, and T. Geisel, Nature **439**, 462 (2006).
[5] D. Brockmann and L. Hufnagel, Phys. Rev. Lett. **98**, 178301 (2007).
[6] C. Song, Z. Qu, N. Blumm, and A. L. Barabási, Science **327**, 1018 (2010), http://www.sciencemag.org/cgi/reprint/327/5968/1018.pdf.
[7] C. Song, T. Koren, P. Wang, and A. L. Barabási, Nat. Phys. **6**, 818 (2010).
[8] F. Simini, M. C. González, A. Maritan, and A. L. Barabási, Nature **484**, 96 (2012).
[9] S. Grauwin, M. Szell, S. Sobolevsky, P. Hövel, F. Simini, M. Vanhoof, Z. Smoreda, A. L. Barabási, and C. Ratti, Sci. Rep. **7**, 46677 (2017).
[10] P. van den Driessche and J. Watmough, Mathematical Biosciences **180**, 29 (2002).
[11] R. Humphries, EpiGraph, `https://github.com/rory-humphries/EpiGraph-cpp` (2020).
[12] Census 2016 Open Data Site, `http://census2016.geohive.ie/datasets/774b6c87f0ec49c48e0e7999fc0e752b_1` (accessed: 17 June 2020).
[13] Census 2016 Profile 6, Commuting in Ireland, `https://www.cso.ie/en/csolatestnews/presspages/2017/census2016profile6-commutinginireland/` (accessed: 17 June 2020).

[14] Northern Ireland Statistics and Research Agency, https://www.nisra.gov.uk/statistics/regional-analysis-and-trends/local-government-district (accessed: 17 June 2020).
[15] (Eurostat, Nomenclature of Territorial Units for Statistics – NUTS, https://ec.europa.eu/eurostat/web/nuts/background.
[16] Department of the Taoiseach and Department of Health: Roadmap for reopening society and business, published at: 1 May 2020, last updated: 12 June 2020, https://www.gov.ie/en/news/58bc8b-taoiseach-announces-roadmap-for-reopening-society-and-business-and-u/, https://assets.gov.ie/73722/ffd17d70fbb64b498fd809dde548f411.pdf (accessed: 17 June 2020).
[17] HRB project: COVID19 rapid response programme (grant number: COV19-2020-117), unpublished data of four waves of telephone surveys.
[18] Health Protection Surveillance Centre (HPSC), https://www.hpsc.ie/a-z/respiratory/coronavirus/novelcoronavirus/casesinireland/ (accessed: June 22, 2020).
[19] Worldometer, https://www.worldometers.info/coronavirus/country/ireland/ (accessed: June 22, 2020).
[20] Central Statistics Office (CSO): Confirmed cases of COVID-19 by Electoral Division, https://census.cso.ie/covid19/.
[21] R. Chowdhury, K. Heng, M. S. R. Shawon, G. Goh, D. Okonofua, C. Ochoa-Rosales, V. Gonzalez-Jaramillo, A. Bhuiya, D. Reidpath, S. Prathapan, *et al.*, European journal of epidemiology **35**, 389 (2020).
[22] G. Killeen and S. Kiware, medRxiv 10.1101/2020.04.15.20066845 (2020), https://www.medrxiv.org/content/early/2020/04/20/2020.04.15.20066845.full.pdf.
[23] S. M. Kissler, C. Tedijanto, E. Goldstein, Y. H. Grad, and M. Lipsitch, Science **368**, 860 (2020).
[24] A. D. Ames, T. G. Molnar, A. W. Singletary, and G. Orosz, medRxiv 10.1101/2020.06.17.20133264 (2020), https://www.medrxiv.org/content/early/2020/06/19/2020.06.17.20133264.full.pdf.
[25] Health Protection Surveillance Centre (HPSC) and the Health Service Executive (HSE): Ireland's COVID-19 Data Hub, https://covid19ireland-geohive.hub.arcgis.com (accessed: 10 July 2020).
[26] R. J. Beverton and S. J. Holt, *On the dynamics of exploited fish populations*, Vol. 11 (Springer Science & Business Media, 1993).
[27] V. Christensen and C. J. Walters, Ecol. Modell. **172**, 109 (2004).
[28] A. Amann, How to choose the best strategy for fighting an infectious disease, private communication (2020).

Appendix A: Next Genration Matrix

We start by splitting the network SIXRD equations (5) into the parts that cause new infections and all other changes. We shall denote the rate of appearance of new infections in compartment U and node i by $\mathcal{F}_{U,i}(x)$. Similarly, let $\mathcal{V}_{U,i}(x)$ be the rate of change of individuals in compartment U and node i by all other means such that $\dot{U}_i = \mathcal{F}_{U,i} - \mathcal{V}_{U,i}$.

This yields the following equations:

$$\mathcal{F}_{S,i} = 0 \tag{A1a}$$

$$\mathcal{F}_{I,i} = \beta c \left(S_i - \frac{S_i}{N_i} \sum_j N_{ij} \right) \frac{I_i + \sum_j \frac{I_j}{N_j} N_{ji} - \frac{I_i}{N_i} \sum_j N_{ij}}{N_i + \sum_j (N_{ji} - N_{ij})} \tag{A1b}$$

$$+ \beta c \frac{S_i}{N_i} \sum_j N_{ij} \frac{I_j + \sum_k \frac{I_k}{N_k} N_{kj} - \frac{I_j}{N_j} \sum_k N_{jk}}{N_j + \sum_k (N_{kj} - N_{jk})}$$

$$\mathcal{F}_{X,i} = 0 \tag{A1c}$$

$$\mathcal{F}_{R,i} = 0 \tag{A1d}$$

$$\mathcal{F}_{D,i} = 0. \tag{A1e}$$

It is an important note that the movement of individuals form I to X does not count as new infections.

$$\mathcal{V}_{S,i} = \beta c \left(S_i - \frac{S_i}{N_i} \sum_j N_{ij} \right) \frac{I_i + \sum_j \frac{I_j}{N_j} N_{ji} - \frac{I_i}{N_i} \sum_j N_{ij}}{N_i + \sum_j (N_{ji} - N_{ij})} \tag{A2a}$$

$$+ \beta c \frac{S_i}{N_i} \sum_j N_{ij} \frac{I_j + \sum_k \frac{I_k}{N_k} N_{kj} - \frac{I_j}{N_j} \sum_k N_{jk}}{N_j + \sum_k (N_{kj} - N_{jk})}$$

$$\mathcal{V}_{I,i} = \mu I + \alpha I + \kappa I \tag{A2b}$$

$$\mathcal{V}_{X,i} = -\kappa I_i + \mu X_i + \alpha X_i \tag{A2c}$$

$$\mathcal{V}_{R,i} = -\mu I_i - \mu X_i \tag{A2d}$$

$$\mathcal{V}_{D,i} = -\alpha I_i - \alpha X_i. \tag{A2e}$$

For the above equations, we replace the coupling variables with their actual values, i.e. we take $S_{ij} = \frac{S_i}{N_i} N_{ij}, I_{ij} = \frac{I_i}{N_i} N_{ij}, \ldots$ etc. Writing these equations in vector form we obtain

$$\mathcal{F} = \begin{bmatrix} \mathcal{F}_{I,1} \\ \vdots \\ \mathcal{F}_{I,n} \\ \mathcal{F}_{X,1} \\ \vdots \\ \mathcal{F}_{X,n} \\ \mathcal{F}_{S,1} \\ \vdots \\ \mathcal{F}_{S,n} \\ \mathcal{F}_{R,1} \\ \vdots \\ \mathcal{F}_{R,n} \\ \mathcal{F}_{D,1} \\ \vdots \\ \mathcal{F}_{D,n} \end{bmatrix}, \quad \mathcal{V} = \begin{bmatrix} \mathcal{V}_{I,1} \\ \vdots \\ \mathcal{V}_{I,n} \\ \mathcal{V}_{X,1} \\ \vdots \\ \mathcal{V}_{X,n} \\ \mathcal{V}_{S,1} \\ \vdots \\ \mathcal{V}_{S,n} \\ \mathcal{V}_{R,1} \\ \vdots \\ \mathcal{V}_{R,n} \\ \mathcal{V}_{D,1} \\ \vdots \\ \mathcal{V}_{D,n} \end{bmatrix}. \tag{A3}$$

The disease-free equilibria are all solutions that satisfy

$$x_0 = (I_0, \ldots, I_n, X_1, \ldots, X_n, S_1, \ldots, S_n, R_1, \ldots, R_n, D_1, \ldots, D_n) \tag{A4}$$
$$= (0, \ldots, 0, 0, \ldots, 0, S_1, \ldots, S_n, R_1, \ldots, R_n, D_1, \ldots, D_n) \tag{A5}$$

Taking the derivatives of $\mathcal{F}$ and $\mathcal{V}$ at the disease-free equilibria, we find that

$$D\mathcal{F}(x_0) = \begin{bmatrix} F & 0 \\ 0 & 0 \end{bmatrix} \quad \text{and} \quad D\mathcal{V}(x_0) = \begin{bmatrix} V & 0 \\ J_1 & J_2 \end{bmatrix} \tag{A6}$$

as shown in [10]. We obtain

$$F_{ij} = \beta c \left[\left(S_i - \frac{S_i}{N_i} \sum_k N_{ik} \right) \frac{\delta_{ij} \left(1 - \sum_k \frac{N_{ik}}{N_i} \right) + \frac{N_{ji}}{N_j}}{N_i + \sum_k (N_{ki} - N_{ik})} + \frac{S_i}{N_i} \sum_k N_{ik} \frac{\delta_{jk} \left(1 - \sum_l \frac{N_{jl}}{N_j} \right) + \frac{N_{jk}}{N_j}}{N_k + \sum_l (N_{lk} - N_{kl})} \right] \tag{A7}$$

$$V_{ij} = (\mu + \alpha + \kappa) \delta_{ij} \tag{A8}$$

Finally, following [10], the next generation matrix is given by

$$FV_{ij}^{-1} = \frac{\beta c}{\mu + \alpha + \kappa} \left[\left(S_i - \frac{S_i}{N_i} \sum_k N_{ik} \right) \frac{\delta_{ij} \left(1 - \sum_k \frac{N_{ik}}{N_i} \right) \frac{N_{ji}}{N_j}}{N_i + \sum_k (N_{ki} - N_{ik})} \right.$$
$$\left. + \frac{S_i}{N_i} \sum_k N_{ik} \frac{\delta_{jk} \left(1 - \sum_l \frac{N_{jl}}{N_j} \right) + \frac{N_{jk}}{N_j}}{N_k + \sum_l (N_{lk} - N_{kl})} \right]. \tag{A9}$$